

1 High-fidelity annotated genome of the polyploid and
2 quarantine root-knot nematode, *Meloidogyne enterolobii*

3

4 **Authors**

5 Marine Pouillet¹, Hemanth Gopal², Corinne Rancurel¹, Marine Sallaberry³, Celine Lopez-
6 Roques³, Joanna Lledo³, Sebastian Kiewnick^{2*}, Etienne GJ Danchin^{1*}

7

8 **Affiliations**

9 1. Institut Sophia Agrobiotech, INRAE, Université Côte d'Azur, CNRS, 400 routes des Chappes,
10 06903 Sophia-Antipolis, France

11 2. Julius Kühn-Institut, Institute for Plant Protection in Field Crops and Grassland, Messeweg
12 11-12, 38104 Braunschweig, Germany

13 3. INRAE, GeT_PlaGe, Genotoul, 31326 Castanet – Tolosan, France. DOI:10.17180/nvxj-5333

14 *These authors jointly supervised this work

15 Corresponding author(s): Marine Pouillet (marine.pouillet@inrae.fr); Etienne G.J Danchin
16 (etienne.danchin@inrae.fr)

17

18 **Abstract**

19 Root-knot nematodes of the genus *Meloidogyne* are obligatory plant endoparasites that cause
20 substantial economic losses to the agricultural production and impact the global food supply.
21 These plant parasitic nematodes belong to the most widespread and devastating genus
22 worldwide, yet few measures of control are available. The most efficient way to control root-
23 knot nematodes (RKN) is deployment of resistance genes in plants. However, current
24 resistance genes that control other *Meloidogyne* species are mostly inefficient on *M.*
25 *enterolobii*. Consequently, *M. enterolobii* was listed as a European Union quarantine pest
26 implementing regulation. To gain insight into the molecular characteristics underlying its
27 parasitic success, exploring the genome of *M. enterolobii* is essential. Here, we report a high-
28 quality genome assembly of *Meloidogyne enterolobii* using the high-fidelity long-read
29 sequencing technology developed by Pacific Biosciences, combined with a gap-aware
30 sequence transformer, DeepConsensus. The resulting genome assembly spans 273 Mbp with
31 556 contigs, a GC% of 30 ± 0.042 and an N50 value of 2.11Mb, constituting a useful platform
32 for comparative, population and functional genomics.

33

34 **Background & Summary**

35 Root-knot nematodes (RKN) belong to the genus *Meloidogyne*, and are among the most
36 destructive plant-parasitic nematodes¹. Due to their extensive geographic distribution and
37 ability to infest a wide range of host plants, they have a detrimental impact on the yield and
38 quality of numerous economically valuable crops². At present, the *Meloidogyne* genus
39 comprises more than 100 described species. However, *M. arenaria*, *M. incognita*, *M. javanica*
40 and *M. hapla* are considered the most widespread and damaging, RKN species³. In recent
41 years, *M. enterolobii* has received increasing attention due to its unique ability to overcome
42 several sources of resistance against RKN^{2,4,5}.

43 The species *Meloidogyne enterolobii* was originally first described as *M. incognita* from a
44 population obtained from the Pacara Earpod Tree (*Enterolobium contortisiliquum* [Vell.]
45 Morong) in Hainan Island, China by Yang and Eisenback (1983)⁶. Later in 1988, Rammah and
46 Hirschmann described a new species⁷, *M. mayaguensis*, sampled from eggplant (*Solanum*
47 *melongena* L.) roots from Puerto Rico. However, this species was later synonymized with *M.*
48 *enterolobii*, based on the same esterase phenotype and mitochondrial DNA sequence^{8,9}.

49 *Meloidogyne enterolobii* has an extremely high damage potential¹⁰, surpassing many of the
50 other root-knot nematode species studied so far^{11,12}. The reports of severe damage in high-
51 value crops have increased in the past years^{13,14}. In 2009, the European Plant Protection
52 Organization (EPPO) performed a risk analysis, which came to the conclusion that this species
53 was recommended for regulation and placed on the EPPO A2 list in 2010. Following numerous
54 interceptions over the years, it was concluded that *M. enterolobii* fulfilled the conditions
55 provided in Article 3 and Section 1 of Annex I to Regulation (EU) 2016/2031 in respect of the
56 Union territory and therefore should be listed in Part A of Annex II to Implementing Regulation
57 (EU) 2019/2072 as Union quarantine pest¹⁵. However, once damage is detected, *M. enterolobii*
58 identification is challenging due to morphological resemblances it shares with other root-knot
59 nematode species^{11,14,16,17}.

60 In that perspective, providing high-quality nuclear and mitochondrial genomes for this species
61 can accelerate the development of reliable molecular markers and the understanding of the
62 biology of *M. enterolobii*. A first version of the genome of *M. enterolobii* was published in 2017
63 as part of a comparative genomics analysis with other root-knot nematodes¹⁸. The population
64 named L30, originated from Burkina Faso and was sequenced using Illumina short reads.
65 Consequently, the assembled genome was quite fragmented with >46,000 contigs and an N50
66 length <9.3kb, precluding analyses of structural variants or conserved synteny with other
67 *Meloidogyne* species. Nevertheless, this initial genome allowed confirming that this species
68 was likely polyploid, similarly to other tropical parthenogenetic root-knot nematodes¹⁹. More

69 recently, a *M. enterolobii* genome assembled from PacBio RS long reads and polished with
70 Illumina short reads was published²⁰. The sequenced population named Mma-II, was isolated
71 from infected tomatoes in a Swiss organic farm²¹. With <4,500 contigs and an N50 length of
72 143kb, the genome assembly represented a substantial improvement compared to the only
73 other assembly available at this time. However, recent progress in the quality and data volume
74 of long-read sequencing technologies²² promises even more contiguous and higher-quality
75 genomes even for complex polyploid species and including the *Meloidogyne* genus^{23,24}.
76 Therefore, we used the PacBio HiFi, highly accurate long-read sequencing technology to
77 produce a more contiguous and reliable reference genome for this quarantine plant-parasitic
78 nematode.

79 Using this technology and further improvement of the quality of the reads, we assembled the
80 genome of the *Meloidogyne enterolobii* population (E1834), originally isolated from the roots
81 of eggplant collected in Puerto Rico, in 556 contigs with an N50 length surpassing 2Mb and a
82 genome assembly size of 273Mb, consistent with previous flow cytometry estimation on a
83 population from Guadeloupe island (274.7 +- 18.52 Mb)²⁰. Compared to the previous long-
84 read version of the genome, this constitutes an improvement of the N50 contiguity by more
85 than one order of magnitude, with the number of contigs divided by almost 10.

86 Further quality check of our genome assembly and comparison with previous assemblies
87 confirmed the correct species identification for population E1834 and for the isolate from
88 Burkina Faso previously sequenced with short reads. However, our study also revealed that
89 the Mma-II Swiss population previously sequenced with PacBio RS underwent a contamination
90 by *M. incognita*, which over several generations in a greenhouse, completely overtook
91 originally described *M. enterolobii* population M-ma-II. As this population was not maintained
92 as a single egg mass line, contamination by a highly virulent and equally pathogenic *M.*
93 *incognita* population remained undetected. Mis-identification among *Meloidogyne* species is
94 not uncommon as reported populations of *M. ethiopica* in Europe were later identified as *M.*
95 *luci*²⁵. Consequently, the genome assembly in that publication²⁰ corresponded to *M. incognita*
96 implying no long-read-based contiguous genome for *M. enterolobii* was finally available so far.
97 This finding also motivated us to develop a methodology based on mitochondrial genomes
98 reconstruction and relative coverage to detect contamination between closely related species
99 which are not detectable with standard Blobtools²⁶ approaches based on contigs GC content
100 and coverage. This methodology can be reused to confirm correct species identification in
101 sequencing projects.

102 Overall, we propose a high-quality contiguous genome for *M. enterolobii* constituting a reliable
103 resource for within- and between-species comparative genomics. The contiguity of the

104 genome enables study of structural variations and conserved synteny, which will be essential
105 towards comprehensive identification of genomic variations in relation with the host range of
106 this quarantine nematode species in Europe.

107

108 **Methods**

109 **Nematode collection and DNA extraction**

110 The *Meloidogyne enterolobii* population (E1834) was originally isolated from the roots of
111 eggplant collected in Puerto Rico and has been maintained since 2005 in the *Meloidogyne* sp.
112 reference collection at The Netherlands Institute for Vectors, Invasive plants and Plant health
113 (NIVIP) Wageningen, Netherlands. In 2020, this population was kindly provided by NRC, for
114 the research conducted in the framework of the project AEGONE (No . 431627824r) and has
115 been maintained at the Julius Kühn Institut (JKI) in Braunschweig, Germany in a greenhouse
116 on the resistant tomato cultivar 'Phantasia'. Nematodes used for DNA extraction were
117 obtained from single egg mass (SEM) lines. To obtain these lines, 12 single females with egg
118 masses were carefully picked from the infected roots of tomato and second stage juveniles
119 (J2) were allowed to hatch in six well plates (SARSTEDT AG & Co. KG, Nümbrecht, DE) with 5ml
120 molecular grade water per well. After one week at room temperature ($20 \pm 1^\circ\text{C}$) in the dark,
121 10 wells with the highest number of hatched J2s were selected for inoculation. In addition,
122 two J2s from each egg mass were collected for DNA extraction and species verification by Real-
123 time PCR²⁷ and SCAR species-specific markers^{28,29}. For multiplication of the SEMs, five-week-
124 old tomato seedlings from the cultivar 'Phantasia' were transplanted into 1000 ml clay pots
125 (Risa Pflanzgefäße GmbH, Germany) containing 750ml quartz sand (0.3-1mm) supplemented
126 with slow-releasing fertilizer, Osmocote (1.5g/L). Afterwards, tomatoes were inoculated with
127 J2s obtained from the respective egg masses. Tomato plants were maintained in a greenhouse
128 at 20 to 25°C with 16h of light and 8h of darkness. Plants were watered daily and fertilized
129 once per week with Wuxal® super solution (8:8:6; N: P: K, Hauert MANNA, Nürnberg, DE). After
130 8 weeks, the galled roots were carefully washed free of sand and the eggs and juveniles (E&J)
131 were extracted with 0.7% chlorine solution³⁰. The resulting E&J suspension was counted to
132 identify the line with the highest reproduction rate. The SEML number 4 was therefore
133 selected (Table 1) for further experiments and production of DNA.

134

135

136

	Number of Egg & Juveniles per root
SEML 1	43,200 ± 577.35
SEML 2	22,7800 ± 1285.82
SEML 3	56,600 ± 1604.16
SEML 4	454,800 ± 1442.22
SEML 5	230,400 ± 945.16
SEML 6	3000 ± 503.32
SEML 7	187,800 ± 2457.64
SEML 8	170,000 ± 416.33
SEML 9	109,000 ± 1222.02
SEML 10	189,800 ± 901.85

137

138 Table 1: Number of newly produced eggs and juveniles per root system of 10 single eggs mass
139 lines of *Meloidogyne enterolobii* population (E1834). Tabulated values are the mean count of
140 Eggs and Juveniles with standard error for different SEML.

141

142 **DNA extraction**

143 The selected SEML 4 was multiplied on tomato plants to obtain J2 for DNA extraction. Galled
144 tomato roots were carefully washed free of sand and placed in a mist chamber to collect
145 freshly hatched J2 after 14 days. The J2 suspension was purified by the modified centrifuge-
146 floatation method³¹ with a 45% sugar solution to reduce contaminations such as root debris,
147 bacteria, fungal spores, etc... Afterwards, approximately 50,000- 70,000 J2 were transferred
148 into 1.5ml Eppendorf tube and washed 3 times with molecular grade water. After freezing in
149 liquid nitrogen, DNA was extracted from the homogenized sample using the MasterPure
150 Complete DNA & RNA Purification Kit (Lucigen) following the manufacturer's protocol. The
151 DNA was suspended in 10mM Tris-HCl buffer and the DNA concentration was determined with
152 either a QubitTM 4 fluorometer (Life Technologies, Singapore) or NanoDrop 2000 TM
153 spectrophotometer (Thermo Fisher Scientific, USA). The NanoDrop 2000TM was blanked using
154 the respective elution buffer for the method. DNA concentration was measured using QubitTM
155 (1X dsDNA HS (High Sensitivity) Assay Kit, Invitrogen, #Q32853) and NanoDrop 2000TM. Purity
156 was measured using the 260/280 nm and 260/230 nm absorbance ratios of NanoDrop 2000TM.

157

158

159

160 **Genome sequencing and read processing**

161 The long-fragment DNA libraries from the *M. enterolobii* population E1834 were constructed
162 at the GeT-PlaGe core facility, INRAE Toulouse according to the manufacturer's instructions
163 "Preparing whole genome and metagenome libraries using SMRTbell® prep kit 3.0". At each
164 step, DNA was quantified using the Qubit dsDNA HS Assay Kit (Life Technologies). DNA purity
165 was tested using the nanodrop (Thermofisher) and size distribution and degradation assessed
166 using the Femto pulse Genomic DNA 165 kb Kit (Agilent). Purification steps were performed
167 using AMPure PB beads (PacBio) and SMRTbell cleanup beads (PacBio). A DNA damage repair
168 step was performed using the « SMRTbell Damage Repair Kit SPV3 » (PacBio). A total of 9.4µg
169 of DNA was purified and then sheared at 20 kb using the Megaruptor system (Diagenode).
170 Using SMRTbell® prep kit 3.0, a Single strand overhangs removal, a DNA and END damage
171 repair step were performed on 8.3µg of sample. Subsequently, blunt hairpin adapters were
172 ligated to the library and a nuclease treatment was performed using the nuclease mix of
173 "SMRTbell® prep kit 3.0". A size selection step using a 6kb cutoff was performed on the
174 BluePippin Size Selection system (Sage Science) with "0.75% DF Marker S1 6-10 kb vs3
175 Improved Recovery" protocol. Using Binding kit 2.2 kit and sequencing kit 2.0, the primer V5
176 annealed and polymerase 2.2 bounded library was sequenced by diffusion loading with the
177 adaptive loading method onto 1 on Sequel II instrument at 90pM with a 2 hours pre-extension
178 and a 30 hours movie.

179 The Sequel II sequencing system outputs 1To of raw data into a subread file. This contains
180 unaligned base calls from high-quality regions, the complete set of base quality values and
181 kinetic measurements from the sequencing instrument. This subread file is used as input for
182 the Circular Consensus Sequencing (CCS v6.4.0) analysis to generate a draft consensus
183 sequence. Very low-quality reads (<Q9) were filtered out by using the parameter --min-
184 rq=0.88. To further improve the quality of the PacBio Sequel II reads, we have used a gap-
185 aware sequence transformer, DeepConsensus³² (v1.1.0). As a final step, the previous subreads
186 were aligned to the draft consensus sequence using ACTC³³ with default parameters (v0.2.0)
187 and used as input to the DeepConsensus transformer-encoder. The Phred-scale read accuracy
188 score (Qconcordance) has been calculated according to Baid et al.³² where Qconcordance = -
189 10*log10 (1-identity) and identity = matches / (matches + mismatches + deletions +
190 insertions).

191

192 **Ploidy, heterozygosity, and genome size estimation**

193 To infer the ploidy level of the *M. enterolobii* population E1834, a k-mer-based approach was
194 employed to profile the genome. The k-mer frequencies in DeepConsensus sequencing reads

195 were analyzed using KMC³⁴ (v3.0.0, `kmc -k21 -m100 -ci1 -cs10000`). In accordance with the
196 author's recommendations, canonical 21-mers were extracted using a hash and organized in
197 a histogram file using the `kmc_tools transform` option. To determine the appropriate coverage
198 thresholds required for the inference, the KMC histogram file is utilized as input for the `cutoff`
199 option in Smudgeplot³⁵ (v0.2.4). Subsequently, we generated a smudge plot using the
200 coverage of the identified k-mer pairs to determine ploidy.

201 To estimate genome size and heterozygosity prior to assembly, we used Genomescope³⁵ (v2.0)
202 on the histogram file generated from Jellyfish³⁶ (v2.3.0, `jellyfish histo -h 1000000`) and the
203 coverage thresholds produced by the Smudgeplot `cutoff` tool. The final genome size is
204 therefore obtained by multiplying the haploid genome size by the previously estimated ploidy
205 level.

206

207 **Genome assembly, estimation of completeness and contamination**

208 DeepConsensus reads were trimmed of remaining adapters using HifiAdapterFilt³⁷ (v2.0.0)
209 with default parameters. The trimmed reads were then used as input to the Peregrine-2021
210 assembler^{38,39} (v0.4.11) while increasing the default number of best overlaps for each initial
211 graph (parameter `--bestn 8`). This parameter is optimized for highly heterozygous genomes.

212 To further assess genome assembly completeness in a reference-free approach, we used
213 Merqury's algorithm⁴⁰ (v1.3). This tool uses k-mer frequencies to evaluate a genome's base
214 accuracy and completeness. This is achieved by counting and comparing the distribution of
215 canonical 21-mers found in the assembled genome with those detected in the high-accuracy
216 DeepConsensus read set. Merqury's k-mer analysis will therefore indicate whether the
217 genome assembly has captured all the information present in the HiFi reads.

218 The screening of the contig assembly for potential contaminants by non-nematode sequences
219 was done with the Blobtools²⁶ pipeline (v3.2.6). DeepConsensus polished long-reads were
220 aligned to the contigs with Minimap2⁴¹ (v2.24) and the `map-hifi` parameter. Each contig was
221 then assigned to a taxonomic group based on the BLAST⁴² (v2.13.0+) analysis results against
222 the NCBI nucleotide (nt) database⁴³. Particular attention was paid to contigs of non-nematode
223 taxa or contigs with a GC percentage deviating from the average GC content (around 30%¹⁸)
224 of the *M. enterolobii* population E1834 to detect possible contamination. A total of 39 contigs
225 spanning ~2.5 Mbp were discarded from the assembly. The resulting assembly of 556 contigs
226 is used for downstream analyses.

227

228

229

230 **Mitochondrion assembly and functional annotation**

231 The circular mitochondrial genome sequence was reconstituted using the ALADIN⁴⁴ package
232 (v1.1) and DeepConsensus HiFi reads in input with default parameters. We employed as a
233 reference seed sequence the complete mitochondrion of *M. enterolobii* previously
234 downloaded from the GenBank database (BioProject: PRJNA927338⁴⁵). The annotation was
235 carried out using GeSeq⁴⁶, encompassing both the tRNA, the rRNA and the protein-coding
236 genes. We set the minimum threshold of 85% for the protein and non-coding DNA search
237 identity, and we used seven *Meloidogyne* mitochondrial genomes as third-party references
238 (Table 2). The tRNAs prediction was also performed using third-party predictors, such as
239 tRNAscan-SE⁴⁷ (v2.0.7), ARAGORN⁴⁸ (v1.2.38), and ARWEN⁴⁹ (v1.2.3), with codon usage
240 corresponding to Metazoan and Invertebrate Mitochondrial.

241

242 **Gene prediction and genome structure determination**

243 Gene models prediction was done with the fully automated pipeline EuGene-EP⁵⁰ (v1.6.5).
244 EuGene has been configured to integrate similarities with known proteins of *Caenorhabditis*
245 *elegans* (PRJNA13758) from WormBase Parasite⁵¹ and “nematoda” section of
246 UniProtKB/Swiss-Prot library⁵², with the prior exclusion of proteins that were similar to those
247 present in RepBase⁵³. The dataset of *Meloidogyne enterolobii* transcribed sequences²⁰ was
248 aligned on the genome and used by EuGene as transcription evidence. Only the alignments of
249 datasets on the genome spanning 30% of the transcript length with at least 97% identity were
250 retained. The EuGene default configuration was edited to set the “preserve” parameter to 1
251 for all datasets, the “gmap_intron_filter” parameter to 1 and the minimum intron length to
252 35 bp. Finally, the Nematodes-specific Weight Array Method matrices were used to score the
253 splice sites (available at this URL: http://eugene.toulouse.inra.fr/Downloads/WAM_nematodes_20171017.tar.gz).

255 Genome structure analysis was conducted using MCSanX⁵⁴, with default settings. First, the
256 whole proteome of the *M. enterolobii* population E1834, predicted by EuGene, was self-
257 blasted with an E-value cutoff of 1e-25, a maximum of 5 aligned sequences, and maximum 1
258 high-scoring pair (hsp). Subsequently, we used gene location information extracted from the
259 GFF3 annotation file of EuGene, along with homology information based on the all-versus-all
260 BLASTP analysis, to identify and categorize each duplicated protein-coding gene into one of
261 five groups using the duplicate_gene_classifier program implemented in the MCSanX
262 package. These groups are: singleton, proximal, tandem, whole-genome or segmental
263 duplications (WGD), and dispersed duplications. Singleton refers to cases where no duplicates

264 are found in the assembly. Proximal duplicates refer to gene duplications that are on the same
265 contig and separated by 1 to 10 genes. Tandem duplicates, on the other hand, are consecutive.
266 WGD are identified when they form collinear blocks with other pairs of duplicated genes.
267 Finally, dispersed duplicates are those that cannot be assigned to any of the above-mentioned
268 categories.

269 **Species verification and validation**

270 In the following step, we further screened the genomic reads for potential contamination, this
271 time by other root-knot nematode sequences. Blobtools allows the identification of potential
272 contamination in genome assemblies, but only at distant taxonomic levels between different
273 phyla (e.g., Chordata, Nematoda, Arthropoda, ...). Therefore, although contamination can be
274 detected and cleaned at this level, it remains undetectable at the intra-phylum level (e.g.
275 within Nematoda). To allow the detection of contamination by other closely related
276 nematodes at the reads level, we adapted the Blobtools pipeline to work with mitochondrial
277 genomes. The polished long-reads were aligned against complete mitochondrial sequences
278 for seven *Meloidogyne* species downloaded from the NCBI database (Table 2), using the same
279 procedure as above. Since Blobtools only works at the phylum and not species rank, we used
280 a script to create an additional hits file and assign a custom NCBI phylum TaxID to each species.
281 The seven *Meloidogyne* samples have been then temporarily assigned to a different phylum
282 for the BlobPlot visualization only (Table 2).

283

Species	Length (bp)	GenBank accession	TaxIDs	Custom TaxIDs
<i>M. graminicola</i> ⁵⁵	19589	NC_056772	189291	4890(Ascomycota)
<i>M. arenaria</i> ⁵⁶	17580	NC_026554	6304	6340 (Annelida)
<i>M. enterolobii</i> ⁴⁵	17053	NC_026555	390850	390850
<i>M. javanica</i> ⁵⁷	18291	NC_026556	6303	10190 (Rotifera)
<i>M. incognita</i> ⁵⁸	17662	NC_02409	6306	6656 (Arthropoda)
<i>M. chitwoodi</i> ⁵⁸	18201	KJ476150	59747	6447 (Mollusca)
<i>M. oryzae</i> ⁵⁹	17066	MK507908	325757	7711 (Chordata)

284

285 Table 2: Mitochondrial sequence data statistics for different nematodes and their
286 correspondence with the modified Blobtools analyses. Seven *Meloidogyne* mitochondrial
287 sequences have been analyzed for this study. For each species, a specific custom TaxID
288 corresponding to a different phylum has been used.

289

290 Species-specific SCAR (sequence characterized amplified region) markers are routinely used to
291 confirm species identity in plant-parasitic nematodes⁶⁰. SCAR markers are locus-specific
292 fragments of DNA that are amplified by PCR using specific 15-30bp primers. In this study, we
293 retrieved primer sequences of species-specific SCAR markers from the literature
294 (Supplementary Table 1) for four Meloidogyne species with genome assemblies publicly
295 available and belonging to the same clade (*M. arenaria*, *M. incognita*, *M. javanica* and *M.*
296 *enterolobii*). We aligned all the primers to all the above-mentioned genomes with BLAST and
297 when the primer pairs matched on the same contig, we retrieved from the genome the 'virtual'
298 PCR products. After verification of consistency with the lengths from the literature, the virtual
299 PCR products were then aligned to the two previous and present versions of *M. enterolobii*
300 genome assemblies with an E-value threshold of 1e-25.

301

302 **Data Records**

303 All the PacBio HiFi sequence data as well as the genome assemblies and gene predictions
304 supporting the results of this paper have been deposited and are publicly available at the
305 EMBL-EBI's European Nucleotide Archive (ENA) under accession number PRJEB69523
306 (<https://www.ebi.ac.uk/ena/browser/view/PRJEB69523>)⁶¹. All the processed data, including
307 genome assemblies⁶², gene predictions⁶³, and all the structural annotation⁶⁴ results have been
308 deposited and are publicly available at the Recherche Data Gouv institutional collection.

309

310 **Technical Validation**

311 **Assessing read accuracy**

312 After implementing the DeepConsensus³² sequence transformer procedure, statistical analysis
313 showed an increase in the number of high-quality reads obtained (Fig. 1, Table 3) with long
314 fragment DNA reads of up to 26kb in length. The average length of the reads is around 11kb
315 with a total number of 2.4M reads, and a higher average Phred-scale read accuracy score
316 (Qconcordance), which increased from 31.95 before to 34 after DeepConsensus. This
317 transformer has elevated the PacBio HiFi read yield to a minimum Q30 by 10% and a minimum
318 Q40 score (99.99% read accuracy) by 70%. Furthermore, we have retrieved 198,880 long-reads
319 that were initially dismissed prior to treatment in the filter, providing us with more chances to
320 comprehensively capture the entire genome of *M. enterolobii*.

321

322

323

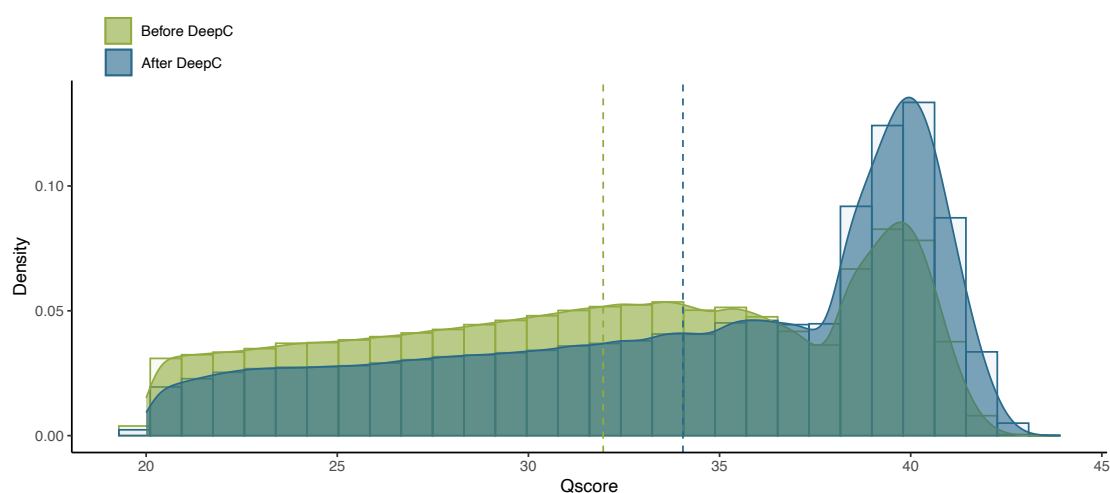
	Before DeepConsensus	After DeepConsensus
Longest read	26 302 bp	26 302 bp
Mean length	11 194 bp	11 187 bp
Number of reads	2 250 199	2 449 079
Number of bases	25 442 730 700	27 277 356 063
Average Qscore	31.95	34.04

324

325 Table 3: Read statistics before and after the use of DeepConsensus sequence transformer.

326 After DeepConsensus treatment, a higher number of reads with higher quality have been
327 retrieved.

328



329

330 **Figure 1.** Distribution of raw PacBio HiFi reads before and after DeepConsensus treatment.

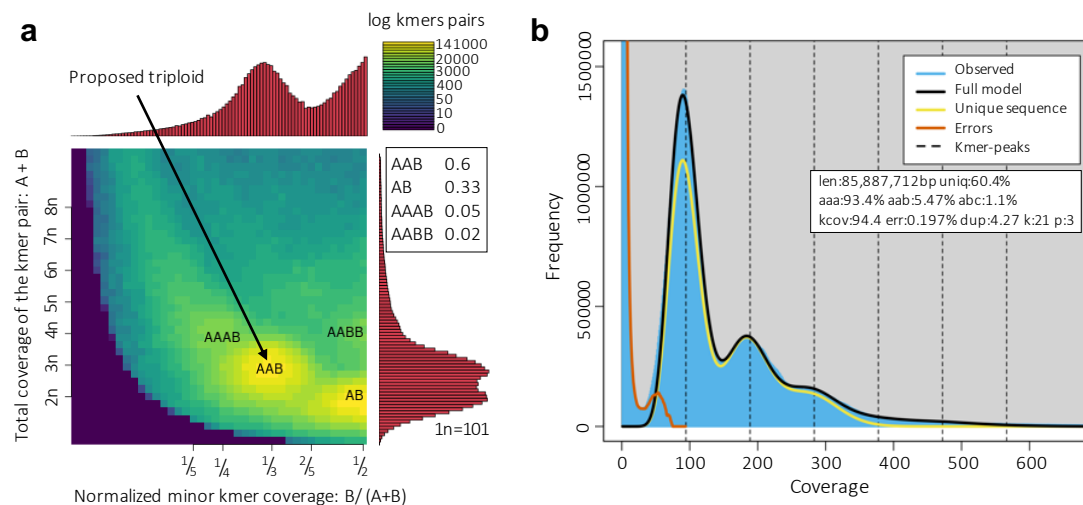
331 Comparison of the Concordance Qscore before and after DeepConsensus. The average phred-
332 scale read accuracy score has increased by two points after treatment.

333

334 Profiling genome ploidy level, heterozygosity, and size.

335 Prior to assembling a genome, it is crucial to evaluate its ploidy and size. The distribution of k-
336 mer frequencies within the DeepConsensus sequencing reads allows estimating major
337 genome features such as ploidy level, genome size, and heterozygosity rate. As
338 GenomeScope2³⁵ can only precisely examine organisms when a definite ploidy is known, we
339 utilized first, the results of Smudgeplot³⁵ (Fig. 2a) to provide GenomeScope2 with estimated
340 ploidy level. Each smudge on the graph appears to be distinct, indicating sufficient sequencing
341 coverage for further analysis. The most prevalent smudge corresponds to a predicted triploid
342 AAB genome for the *M. enterolobii* population E1834 (Table 4). This result is consistent with

343 previous k-mer analysis performed on the short-reads for the L30 population from Burkina
 344 Faso^{18,65}.
 345 Subsequently, we estimated the genome size using GenomeScope2 with a ploidy level of 3
 346 (Fig. 2b). The genome size was determined by multiplying the estimated haploid genome
 347 length (85,887,712 bp) by the previously estimated ploidy level ($p=3$), providing an estimated
 348 genome size of 257.66 Mb.
 349 Furthermore, the GenomeScope2 k-mer histogram of this polyploid population displays a
 350 distinct multimodal profile, with a substantial first peak located at roughly 95X, a smaller
 351 second peak at about 187X, and finally, an additional peak at 282X, typical for triploid
 352 genomes. Finally, GenomeScope2 estimated a highly heterozygous genome (6.5 % estimated
 353 on average), consistent with a previous estimation of ca. 6.1% on the L30 population from
 354 Burkina Faso¹⁸. It should be noted that the term heterozygosity does not exactly apply here as
 355 we do not measure divergence between homologous chromosomes in a diploid genome but
 356 between the AAB subgenomes in a triploid species. Therefore, we will refer to average
 357 nucleotide divergence between subgenomes in the rest of the manuscript.
 358



359
 360 **Figure 2.** Genome profiling of *M. enterolobii*. **A.** Smudgeplot of *M. enterolobii* extracting 21-
 361 mers from DeepConsensus reads. The color intensity of each smudge reflects the approximate
 362 number of k-mers per bin. *M. enterolobii* E1834 population is proposed as a triploid organism.
 363 **B.** GenomeScope2 k-mer profile and estimated parameters for the triploid nematode *M.*
 364 *enterolobii*. Coverage (kcov), error rate (err.), haploid genome size estimation (len.), k-mer size
 365 (k) and ploidy level (p). The peak heights are proportional to the species' heterozygosity. *M.*
 366 *enterolobii* shows a high heterozygosity.
 367

Peak	Kmers #	Kmers proportion	Summit B/ (A+B)	Summit A+B
AAB	5 952 405	0.60	0.34	309.70
AB	3 243 405	0.33	0.49	191.27
AAAB	508 560	0.05	0.24	451.82
AABB	213 490	0.02	0.49	404.45

368 Table 4. Summary of peaks detected by Smudgeplot. This result proposes that the *M.*
369 *enterolobii* E1834 population is triploid.

370

371 ***De novo* genome assembly**

372 After filtering and elimination of the contaminated and mitochondrial contigs, the resulting
373 genome of the *Meloidogyne enterolobii* population E1834 is assembled in 556 contigs with a
374 total size of 273 Mbp. The corresponding contig N50 length is equal to 2.11Mb, with the
375 longest being 8.3 Mb, long.

376 The genome assembly size is congruent with the total DNA content estimated by flow
377 cytometry (274.69 ± 18.52 Mb) on another population of *M. enterolobii* from Guadeloupe
378 island²⁰, indicating that the assembly represents a complete *M. enterolobii* genome.

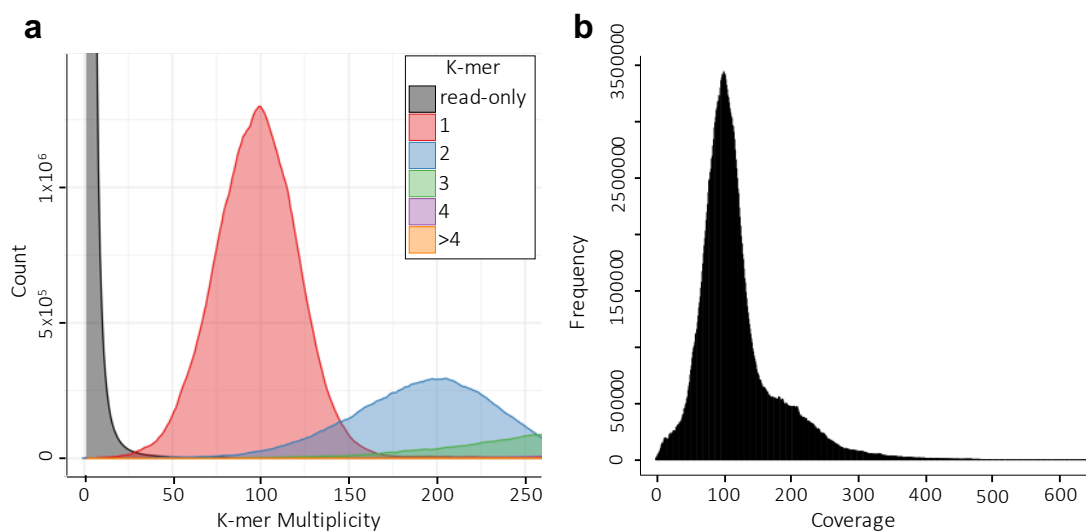
379 However, the genome size estimated by analysis of k-mer distribution (257.66 Mb) is lower
380 than the assembly size and in the lower range of the flow cytometry evaluation. A previous
381 study showed that the accuracy of genome size estimation based on k-mer frequencies can be
382 affected by repeats, high heterozygosity and sequencing errors⁶⁶. This suggests that the high
383 heterozygosity rate or repeat-richness in the *M. enterolobii* genome could have played a role
384 in this underestimation.

385 To further assess genome assembly quality metrics and evaluate genome's base accuracy and
386 completeness we used Merqury⁴⁰. In the Merqury spectrum produced (Fig. 3a), the first and
387 prominent 1-copy peak at a ~100X multiplicity corresponds to k-mers in the reads detected
388 only one time in the assembly. This can be interpreted as heterozygous regions between the
389 three subgenomes. The second peak at twice this multiplicity (~200X) corresponds to
390 homozygous k-mers present in the reads and detected two times in the assembly. This most
391 likely represents regions identical between two of the three AAB subgenomes. Similarly, most
392 of the k-mers detected at 3 times in the assembly, probably represent regions identical
393 between the three AAB subgenomes. Conversely, the grey peak at low multiplicity represents
394 rare k-mers which solely exist within the read set and are probably due to sequencing errors.
395 This Merqury plot indicates a lack of missing content as there is no subsequent grey peak at
396 the 1-copy peak (~100X coverage). Additionally, the AAB subgenomes are divergent enough
397 to have been mostly separated (or unzipped) during the assembly, as there is no smaller

398 second grey peak beneath the 2-copy peak at twice the coverage (~200X). This can also be
399 observed in the coverage plot provided by bedtools⁶⁷ v2.29.0 (Fig. 3b), where the coverage
400 depth for each base on each contig has been computed. We can clearly see a prominent peak
401 located at roughly 101X corresponding to the haploid coverage found in the k-mers with
402 Smugeplot (Fig. 2a), and a shoulder at roughly twice the haploid coverage probably
403 represented few identical regions between sub-genomes that have not been completely
404 unzipped during assembly.

405 Overall, the k-mer analysis with Merqury indicates that all the information present in the HiFi
406 reads has been captured in the genome assembly, further suggesting a complete genome.

407



408

409 **Figure 3.** Genome assembly spectra. **A.** The Merqury spectrum plot using DeepConsensus
410 reads tracks the multiplicity of each k-mer detected in the read set. The plot is color-coded
411 according to the number of times a k-mer is found in an assembly. **B.** Bedtools per-base reports
412 coverage for the assembly. The three *M. enterolobii* AAB subgenomes were effectively
413 separated during assembly using Peregrine.

414

415 **Validating species identity and purity**

416 We confirmed the purity of the *M. enterolobii* population E1834 and the correct species
417 identification by using, first, the Blobtools²⁶ pipeline. The pipeline generated BlobPlots, which
418 are two-dimensional plots depicting contigs presented as circles, whose diameters are
419 proportional to the sequence length and are colored based on their taxonomic affiliation,
420 determined by the BLAST similarity search results against the NCBI nt database⁴³. The relative
421 positions of the circles are according to their GC content and coverage by the long reads.
422 Following the removal of contaminant contigs, the resulting BlobPlot is shown in Figure 4a.

423 Any contigs lacking taxonomic annotation are labeled as 'no-hit'. For the non-Nematoda
424 contigs falling perfectly inside the range of *M. enterolobii* GC content estimates¹⁸ (around
425 30%), a manual verification was conducted and eight of these contigs were kept. The proposed
426 assignments from Blobtools were disregarded. Instead, for each of them we retained the
427 highest-ranking result proposed by BLAST if the calculated percentage of identity surpassed
428 90%, the e-value did not exceed $1e^{-50}$, and the taxID belonged to the Nematoda phylum. This
429 resulted in 556 final contigs for this assembly.

430 The Blobtools pipeline is a valuable tool for detecting possible contaminations in a genome
431 assembly, especially those originating from distant species of different phyla. However, if the
432 contamination comes from a closely related species with a comparable GC content or has been
433 sequenced at a similar coverage, the classical approach will not detect a contamination. For
434 this reason, we made slight adjustments to the methodology (Methods) to achieve a
435 taxonomic classification based on different species within the Nematoda phylum, instead of
436 between phyla only (Fig. 4b, 4c). We focused our analysis on different species within the
437 *Meloidogyne* genus because (i) they are difficult to differentiate based on the morphology, (ii)
438 they live in the same environment, (iii) they have similar GC content. Therefore, a non-
439 negligible possibility for undetected contamination exists.

440 Using this modified BlobTools methodology, on the *M. enterolobii* population E1834 we have
441 sequenced, we observed that the *M. enterolobii* reference mitochondrial genome from the
442 NCBI was highly covered whereas all the other mitochondrial genomes from the other
443 *Meloidogyne* species were not covered by our long reads. Hence, no evidence for
444 contamination by other *Meloidogyne* species was found in the E1834 population (Fig. 4b).

445 For comparison, this method was applied to the previous long-read genome of *M.*
446 *enterolobii*²⁰, and surprisingly, it was found to be heavily contaminated by another
447 *Meloidogyne* (Fig. 4c). Specifically, the *M. enterolobii* mitochondrial genome was not covered
448 by the previous long reads while those of *M. incognita*, *M. javanica* and *M. arenaria* were all
449 substantially covered. Approximately 60%, 30%, and 10% of the mitochondrial reads aligned
450 with these mitochondrial genomes, respectively. Although this adjusted Blobtools approach
451 suggested contamination of the previous Mma-II Swiss population from other root-knot
452 nematodes, this alone was not sufficient to discriminate between these three closely related
453 species.

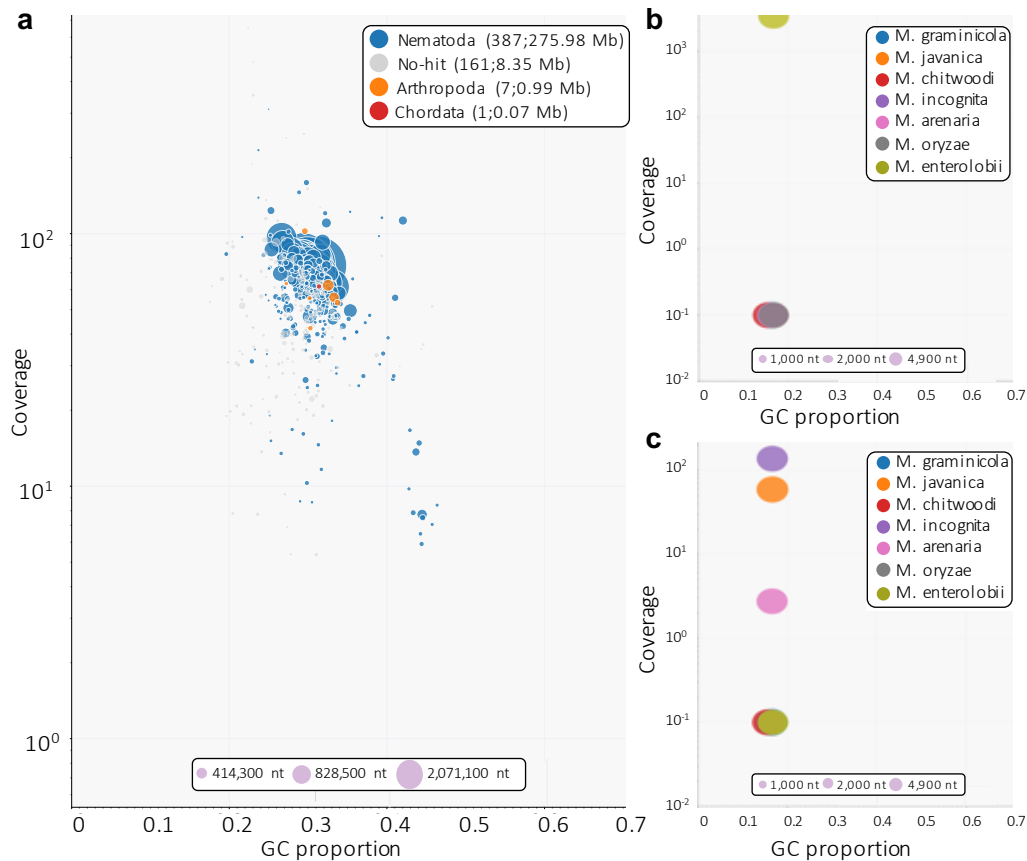
454 Consequently, we combined this approach with SCAR markers. All the pairs of primers for the
455 SCAR marker of the four *Meloidogyne* species of interest were aligned to the previous and
456 current assemblies of *M. enterolobii*. Both for the L30 population of Burkina Faso and the
457 E1834 population from Puerto Rico sequenced here, the pair of primers for the *M. enterolobii*

458 SCAR marker matched the genome assemblies with 100% identity in the correct orientation
459 on one single contig. This allowed identification of a virtual amplified sequence of 537bp,
460 which is consistent with the ~520bp estimated PCR product on the electrophoresis gel in
461 Tigano et al²⁸. In contrast, neither the *M. enterolobii* SCAR primers nor the reconstructed
462 corresponding PCR product matched the previous Mma-II genome assembly, confirming the
463 genome was probably not *M. enterolobii*. To further determine the possible source of
464 contamination, we aligned the pairs of primers of the *M. incognita*, *M. javanica* and *M.*
465 *arenaria* SCAR markers on the Mma-II genome. The *M. incognita* pair of primers matched
466 perfectly on this previous assembly in the correct orientation and allowed reconstructing a
467 virtual PCR product of 1192 bp, consistent with the estimated size of the PCR product of ~1,200
468 bp for *M. incognita*⁶⁰. Neither the pair of *M. incognita* primers nor the reconstructed PCR
469 product matched the L30 or E1834 genome assemblies, and none of the *M. javanica* or *M.*
470 *arenaria* pairs of primers matched any of the previously published or current *M. enterolobii*
471 genomes.

472 Therefore, we can conclude that although no trace of contamination by closely related
473 Meloidogyne species could be identified in the L30 or E1834 genome, there is clear evidence
474 that the Mma-II population had been contaminated and replaced by *M. incognita*.

475 The combination of SCAR marker analysis and a modification of Blobtools, specifically for
476 'mitochondrion', has resulted in a powerful tool for the examination and the verification of
477 species purity.

478



479

480 **Figure 4.** BlobPlot of different *Meloidogyne* genome assemblies. **A.** Blobplot showing
481 taxonomic affiliation at the phylum rank level for the E1834 population of *M. enterolobii*. After
482 removing contamination and mitochondrion, 556 contigs were left. The average GC content
483 for *M. enterolobii* is equal to 30 ± 0.042 . **B.** Mitochondrion only for the E1834 population,
484 after removing contamination. No sign of other Nematoda within the assembly. **C.**
485 Mitochondrion only for the previous *M. enterolobii* reference population provided by
486 Koutsovoulos et al.²⁰. No sign of *M. enterolobii* within the assembly. This BlobPlot revealed a
487 contamination by other *Meloidogyne* spp..

488

489 **Genome completeness assessment**

490 To evaluate the completeness of our genome assembly in terms of expected gene content
491 among related species, we benchmarked nearly universal single-copy orthologs (BUSCO⁶⁸
492 v5.2.2) by using the eukaryote_odb10 lineage dataset in fast mode. Despite the presence of a
493 nematode dataset in BUSCO, it only contains seven species and none of them belong to the
494 same clade as the root-knot nematodes. Therefore, we decided to use the more
495 comprehensive Eukaryotic dataset, which encompasses 70 species. This procedure generates
496 a report that indicates the number of genes that are universally or mostly conserved within
497 the assembly and classifies them into several groups: complete, fragmented, single-copy, or

498 duplicated. The results show that 71.4% (182/255) of BUSCO genes are complete and 12.5%
499 are fragmented. This is a substantial improvement compared to the previously available
500 assemblies (Table 5). Indeed, the Burkina Faso isolate of *M. enterolobii* reached eukaryotic
501 BUSCO completeness score of 59.2% while the Mma-II assembly contaminated by *M. incognita*
502 reached 69.4%.

503 BUSCO is a valuable and robust tool for assessing completeness in a genome assembly in terms
504 of a widely conserved gene set. Nevertheless, in the case of less studied species, the analysis
505 may lack precision if the newly assembled genome comprises variations not included in the
506 initial BUSCO gene set, such as true copy number or sequence variants⁴⁰. We then used
507 Merqury once more to identify any copy-number errors and measure completeness and base
508 accuracy via k-mers. Consequently, Merqury determined the proportion of reliable k-mers in
509 the sequencing sample that were detected in the assembly, resulting in a completeness score
510 of 99.60%. To establish Merqury's base accuracy score, a binomial model for k-mer survival
511 was employed, resulting in a Qscore of 65.70. Higher Qscores indicate a more precise
512 consensus. For instance, Q30 corresponds to an accuracy of 99.9%, Q40 to 99.99%, and so on.
513 In contrast, Burkina Faso and Swiss isolates have Qscores of 55.12 and 29.93, based
514 respectively on their own reads.

515

BUSCO Categories	<i>M. enterolobii</i> (L30 ⁶⁹)	<i>M. enterolobii</i> * (Swiss ²⁰)	<i>M. enterolobii</i> (E1834) **
Complete	59.2% (151)	69.4% (177)	71.4% (182)
Single-copy	29.8% (76)	12.5% (32)	14.9% (38)
Duplicated	29.4% (75)	56.9% (145)	56.5% (144)
Fragmented	18.4% (47)	13.3% (34)	12.5% (32)
Missing	22.4% (57)	17.3% (44)	16.1% (41)

516 Table 5. Ortholog BUSCO completeness analysis for different *M. enterolobii* using lineage
517 dataset eukaryota_odb10. *Population contaminated by *M. incognita*. **This work.

518

519 Gene prediction

520 Using the automated Eugene-EP pipeline, a total of 49,870 genes were predicted, with 45,924
521 being protein-coding genes and 3,946 being non-protein-coding genes such as rRNA, tRNA,
522 and splice leader genes. These genes cover 84 Mb (approximately 29.48%) of the genome
523 assembly length, with the exons spanning 44.51 Mb (around 15.60%). On average, 5.26 exons
524 are predicted per gene, and the gene length varies from a minimum of 150 bp to a maximum
525 of 35,976 bp. The mean GC content is higher in either the protein-coding region (35.19%) or

526 in the non-protein-coding gene regions (44.19%) compared to that of the whole genome
527 (30.34%).

528

529 **Confirmation of genome structure and ploidy level**

530 Although the *M. enterolobii* population E1834 genome has been predicted as a putative
531 triploid based on k-mer analyses and Smudgeplot, it is important to further confirm the ploidy
532 level of the genome assembly after annotation. The use of MCScanX reveals that a majority of
533 gene duplicates create whole duplicated blocks, rather than dispersed independent
534 duplications. Following the classification established by the duplicate_gene_classifier program
535 implemented in the MCScanX package, 39,532 of the protein-coding genes (around 86.10%)
536 are predicted to be duplicated at least once. As evidenced by Table 6, a majority of these
537 coding genes (75.6%) show a duplication depth of two (meaning for these genes, two other
538 copies exist), further reinforcing the idea that the genome is triploid. Furthermore, it was
539 found that 69.76% of the protein-coding genes fall under the whole-genome duplication
540 category of MCScanX, forming 516 syntenic blocks of collinear genes (see Fig. 5 for
541 visualization of multiple syntenic blocks between different contigs). In addition, 12.61% of the
542 genes are classified as dispersed duplicates, while 2.18% and 1.53% constitute proximal and
543 tandem duplicates, respectively. These findings strongly suggest that the genome of *M.*
544 *enterolobii* is triploid, confirming SmudgePlot results.

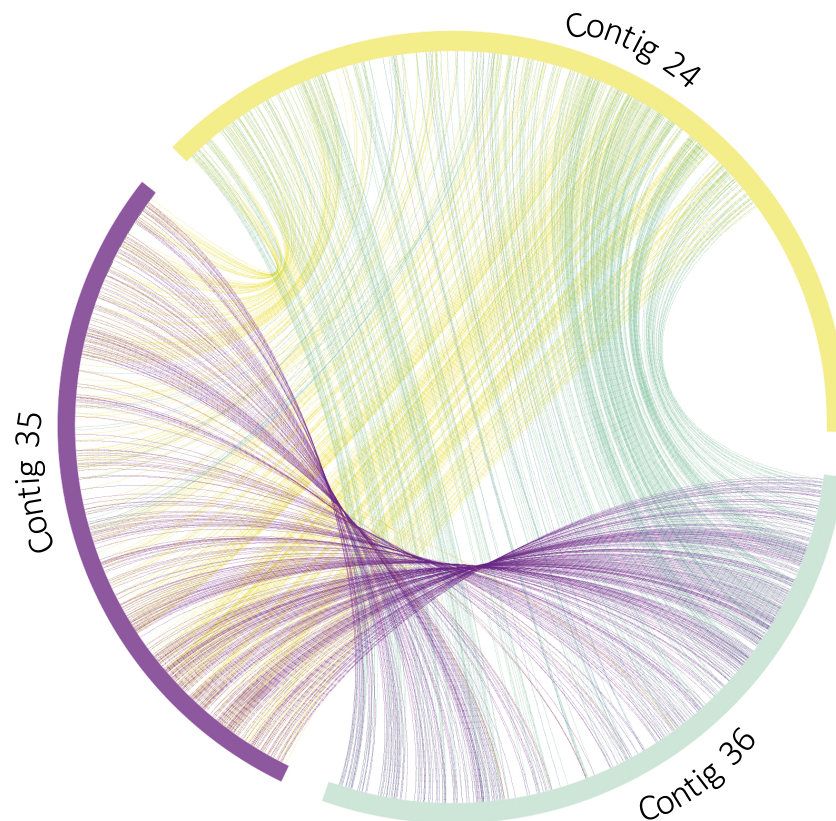
545

Duplication depth	0	1	2	3	4	5+
Gene numbers	1992	4917	34720	2700	769	826
Percentage (%)	4.34	10.71	75.60	5.88	1.67	1.80

546

547 Table 6. Duplicate gene classifier program of MCScanX for a self-comparison of *M. enterolobii*.
548 Genes with a duplication depth of 0 are not duplicated, while a depth of 1 indicates a maximum
549 of one copy, a depth of 2 indicates two copies, and so forth.

550



551

552 **Figure 5.** *M. enterolobii* exhibits a triploid genome. The circle plot produced by MCScanX shows
553 collinear gene pairs forming homologous duplicated regions between three contigs. All the
554 collinear gene pairs are linked with different curved colored lines between and within each
555 contig.

556

557 **Mitochondrial genome assembly and annotation**

558 Using the Aladin package⁴⁴, the mitochondrial genome of the *Meloidogyne enterolobii*
559 population E1834 has been assembled and spanned a length of 19,193 bp with a GC content
560 of 17.2% (Fig. 6). We have retrieved and annotated all the mitochondrially encoded subunits
561 involved in the Mitochondrial respiratory chain, including the seven core subunits of the
562 complex I, the cytochrome b of the complex III, the three cytochrome c, and the ATP synthase.
563 We also obtained a full set of tRNAs, among which were in multiple copies (Ala, Ser, Leu and
564 Asn) as well as ribosomal RNAs (rrnS, rrn12 and rrn16).

565 When blasted against the NCBI nt database, the reconstructed mitochondrial genome of the
566 *Meloidogyne enterolobii* population E1834 returned as first hit the complete mitochondrial
567 reference genome of *M. enterolobii*⁴⁵, with 99.526% identity and an alignment length of
568 13,067 bp, as the primary hsp. The second-best hit corresponds to an incomplete
569 mitochondrial genome from an *M. enterolobii* isolate discovered on sweet potatoes in the
570 state of Carolina in the USA (GenBank: MW246173.1).

585 **Acknowledgements**

586 We are grateful to the colleagues from the Netherlands Institute for Vectors, Invasive Plants
587 and Plant Health (NIVIP) for providing the *M. enterolobii* population E1834 for this study. We
588 thank the genotoul bioinformatics platform Toulouse Occitanie (Bioinfo Genotoul,
589 <https://doi.org/10.15454/1.5572369328961167E12>) for providing computing resources. We
590 are grateful to the bioinformatics and genomics platform, BIG, Sophia Antipolis (ISC plantBIOs,
591 <https://doi.org/10.15454/qyey-ar89>) for computing and storage resources. We thank Claire
592 Caravel for help in providing the primer sequences for SCAR identification of *Meloidogyne*
593 species. Our *M. enterolobii* genome research is financially supported by a Franco-German
594 bilateral grant ANR-DFG “AEGONE”, reference ANR-19-CE35-0017 and reference No
595 431627824.

596

597 **Author contributions**

598 E.G.J.D. and S.K. conceived the research idea and acquired the funding. E.G.J.D. supervised all
599 the bioinformatics analyzes, performed SCAR marker virtual PCRs, contributed to manuscript
600 writing and reviewing. S.K. supervised all the nematode rearing and DNA extraction
601 experiments, contributed to manuscript writing and reviewing. M.P. performed reads
602 processing, genome assembly, contamination and purity check, completeness assessment,
603 ploidy and genome size and structure estimation and wrote the manuscript. H.G. generated
604 single egg mass lines, performed maintenance of the nematode collection, DNA extraction
605 experiments, and contributed to manuscript writing. C.R. performed gene prediction and
606 wrote the corresponding method section. M.S., C.L.R., and J.L. performed library and PACBIO
607 HiFi sequencing and contributed to manuscript writing.

608

609 **Competing interests**

610 The authors declare no competing interests.

611

612 **References**

- 613 1. Jones, J. T. *et al.* Top 10 plant-parasitic nematodes in molecular plant pathology.
614 *Molecular Plant Pathology* **14**, 946–961 (2013).
- 615 2. Santos, D., Abrantes, I. & Maleita, C. The quarantine root-knot nematode *Meloidogyne*
616 *enterolobii* – a potential threat to Portugal and Europe. *Plant Pathology* **68**, 1607–1615 (2019).
- 617 3. Moens, M., Perry, R. N. & Starr, J. L. *Meloidogyne* species - a diverse group of novel
618 and important plant parasites. in (eds. Perry, R. N., Starr, J. L. & Moens, M.) 1–17 (CABI
619 International, Wallingford, Oxon (CABI), 2009).

- 620 4. Kiewnick, S., Dessimoz, M. & Franck, L. Effects of the Mi-1 and the N root-knot
621 nematode-resistance gene on infection and reproduction of *Meloidogyne enterolobii* on tomato
622 and pepper cultivars. *J Nematol* **41**, 134–139 (2009).
- 623 5. Elling, A. A. Major Emerging Problems with Minor *Meloidogyne* Species.
624 *Phytopathology*® **103**, 1092–1102 (2013).
- 625 6. Yang, B. & Eisenback, J. D. *Meloidogyne enterolobii* n. sp. (Meloidogynidae), a Root-
626 knot Nematode Parasitizing Pacara Earpod Tree in China. *J Nematol* **15**, 381–391 (1983).
- 627 7. Rammah, A. & Hirschmann, H. *Meloidogyne mayaguensis* n. sp. (Meloidogynidae), a
628 Root-knot Nematode from Puerto Rico. *J Nematol* **20**, 58–69 (1988).
- 629 8. Karssen, G., Liao, J., Kan, Z., van Heese, E. Y. & den Nijs, L. J. On the species status
630 of the root-knot nematode *Meloidogyne mayaguensis* Rammah & Hirschmann, 1988. *Zookeys*
631 67–77 (2012) doi:10.3897/zookeys.181.2787.
- 632 9. Xu, J., Liu, P., Meng, Q. & Long, H. Characterisation of *Meloidogyne* species from
633 China using Isozyme Phenotypes and Amplified Mitochondrial DNA Restriction Fragment
634 Length Polymorphism. *European Journal of Plant Pathology* **110**, 309–315 (2004).
- 635 10. Sikandar, A., Jia, L., Wu, H. & Yang, S. *Meloidogyne enterolobii* risk to agriculture,
636 its present status and future prospective for management. *Front. Plant Sci.* **13**, 1093657 (2023).
- 637 11. Castagnone-Sereno, P. *Meloidogyne enterolobii* (= *M. mayaguensis*): profile of an
638 emerging, highly pathogenic, root-knot nematode species. *Nematology* **14**, 133–138 (2012).
- 639 12. Castillo, P. & Castagnone-Sereno, P. *Meloidogyne enterolobii* (Pacara earpod tree root-
640 knot nematode). *CABI Compendium CABI Compendium*, 33238 (2020).
- 641 13. Schwarz, T., Li, C., Ye, W. & Davis, E. Distribution of *Meloidogyne enterolobii* in
642 Eastern North Carolina and Comparison of Four Isolates. *Plant Health Progress* **21**, 91–96
643 (2020).
- 644 14. Philbrick, A. N., Adhikari, T. B., Louws, F. J. & Gorny, A. M. *Meloidogyne enterolobii*,
645 a Major Threat to Tomato Production: Current Status and Future Prospects for Its Management.
646 *Frontiers in Plant Science* **11**, (2020).
- 647 15. THE EUROPEAN COMMISSION. COMMISSION IMPLEMENTING
648 REGULATION (EU) 2021/2285 of 14 December 2021 amending Implementing Regulation
649 (EU) 2019/2072 as regards the listing of pests, prohibitions and requirements for the
650 introduction into, and movement within, the Union of plants, plant products and other objects,
651 and repealing Decisions 98/109/EC and 2002/757/EC and Implementing Regulations (EU)
652 2020/885 and (EU) 2020/1292. *Official Journal of the European Union*
653 doi:10.2903/j.efsa.2011.2186.
- 654 16. Blok, V. C. & Powers, T. O. Biochemical and molecular identification. *Root-knot*
655 *nematodes* 98–118 (2009) doi:10.1079/9781845934927.0098.
- 656 17. Min, Y. Y., Toyota, K. & Sato, E. A novel nematode diagnostic method using the direct

- 657 quantification of major plant-parasitic nematodes in soil by real-time PCR. *Nematology* **14**,
658 265–276 (2012).
- 659 18. Szitenberg, A. *et al.* Comparative Genomics of Apomictic Root-Knot Nematodes:
660 Hybridization, Ploidy, and Dynamic Genome Change. *Genome Biol Evol* **9**, 2844–2861 (2017).
- 661 19. Blanc-Mathieu, R. *et al.* Hybridization and polyploidy enable genomic plasticity
662 without sex in the most devastating plant-parasitic nematodes. *PLOS Genetics* **13**, e1006777
663 (2017).
- 664 20. Koutsovoulos, G. D. *et al.* Genome assembly and annotation of *Meloidogyne*
665 *enterolobii*, an emerging parthenogenetic root-knot nematode. *Sci Data* **7**, 324 (2020).
- 666 21. Kiewnick, S., Karssen, G., Brito, J. A., Oggenfuss, M. & Frey, J.-E. First Report of
667 Root-Knot Nematode *Meloidogyne enterolobii* on Tomato and Cucumber in Switzerland. *Plant*
668 *Disease* **92**, 1370–1370 (2008).
- 669 22. Marx, V. Method of the year: long-read sequencing. *Nat Methods* **20**, 6–11 (2023).
- 670 23. Mota, A. P. Z. *et al.* Unzipped genome assemblies of polyploid root-knot nematodes
671 reveal unusual and clade-specific telomeric repeats. *Nat Commun* **15**, 773 (2024).
- 672 24. Dai, D. *et al.* Unzipped chromosome-level genomes reveal allopolyploid nematode
673 origin pattern as unreduced gamete hybridization. *Nat Commun* **14**, 7156 (2023).
- 674 25. Gerič Stare, B., Strajnar, P., Susič, N., Urek, G. & Širca, S. Reported populations of
675 *Meloidogyne ethiopica* in Europe identified as *Meloidogyne luci*. *Plant Disease* **101**, 1627–
676 1632 (2017).
- 677 26. Laetsch, D. R. & Blaxter, M. L. BlobTools: Interrogation of genome assemblies.
678 Preprint at <https://doi.org/10.12688/f1000research.12232.1> (2017).
- 679 27. Kiewnick, S., Frey, J. E. & Braun-Kiewnick, A. Development and Validation of LNA-
680 Based Quantitative Real-Time PCR Assays for Detection and Identification of the Root-Knot
681 Nematode *Meloidogyne enterolobii* in Complex DNA Backgrounds. *Phytopathology*® **105**,
682 1245–1249 (2015).
- 683 28. Tigano, M. *et al.* Genetic diversity of the root-knot nematode *Meloidogyne enterolobii*
684 and development of a SCAR marker for this guava-damaging species. *Plant Pathology* **59**,
685 1054–1061 (2010).
- 686 29. Ye, W., Zeng, Y. & Kerns, J. Molecular Characterisation and Diagnosis of Root-Knot
687 Nematodes (*Meloidogyne* spp.) from Turfgrasses in North Carolina, USA. *PLOS ONE* **10**,
688 e0143556 (2015).
- 689 30. Gómez-González, G. *et al.* *Meloidogyne enterolobii* egg extraction in NaOCl versus
690 infectivity of inoculum on cucumber. *J Nematol* **53**, e2021-57 (2021).
- 691 31. Jenkins, W. R. A rapid centrifugal-flotation technique for separating nematodes from
692 soil. *Plant Dis. Rep.* 48:692, 1964.
- 693 32. Baid, G. *et al.* DeepConsensus improves the accuracy of sequences with a gap-aware

- 694 sequence transformer. *Nat Biotechnol* **41**, 232–238 (2023).
- 695 33. Töpfter, A. PacificBiosciences/ACTC: Align subreads to CCS reads. Available at:
696 <https://github.com/PacificBiosciences/actc>. PacBio (2022).
- 697 34. Kokot, M., Długosz, M. & Deorowicz, S. KMC 3: counting and manipulating k-mer
698 statistics. *Bioinformatics* **33**, 2759–2761 (2017).
- 699 35. Ranallo-Benavidez, T. R., Jaron, K. S. & Schatz, M. C. GenomeScope 2.0 and
700 Smudgeplot for reference-free profiling of polyploid genomes. *Nat Commun* **11**, 1432 (2020).
- 701 36. Marçais, G. & Kingsford, C. A fast, lock-free approach for efficient parallel counting
702 of occurrences of k-mers. *Bioinformatics* **27**, 764–770 (2011).
- 703 37. Sim, S. B., Corpuz, R. L., Simmonds, T. J. & Geib, S. M. HiFiAdapterFilt, a memory
704 efficient read processing pipeline, prevents occurrence of adapter sequence in PacBio HiFi reads
705 and their negative impacts on genome assembly. *BMC Genomics* **23**, 157 (2022).
- 706 38. Chin, J. Peregrine-2021: A faster and minimum genome assembler. (2023).
- 707 39. Chin, C.-S. & Khalak, A. Human Genome Assembly in 100 Minutes. 705616 Preprint
708 at <https://doi.org/10.1101/705616> (2019).
- 709 40. Rhie, A., Walenz, B. P., Koren, S. & Phillippy, A. M. Merqury: reference-free quality,
710 completeness, and phasing assessment for genome assemblies. *Genome Biology* **21**, 245 (2020).
- 711 41. Li, H. New strategies to improve minimap2 alignment accuracy. *Bioinformatics* **37**,
712 4572–4574 (2021).
- 713 42. McGinnis, S. & Madden, T. L. BLAST: at the core of a powerful and diverse set of
714 sequence analysis tools. *Nucleic Acids Res* **32**, W20–W25 (2004).
- 715 43. Sayers, E. W. *et al.* Database resources of the National Center for Biotechnology
716 Information. *Nucleic Acids Res* **50**, D20–D26 (2021).
- 717 44. Koutsovoulos, G. GDKO/Aladin: Aladin (mitochondrial circular DNA reconstitution).
718 Available at: <https://github.com/GDKO/aladin>. GitHub (2021).
- 719 45. Humphreys-Pereira, D. A. & Elling, A. A. *Meloidogyne enterolobii* mitochondrion,
720 complete genome. Available at: https://www.ncbi.nlm.nih.gov/nuccore/NC_026555.1. NCBI.
721 National Center for Biotechnology Information (2015).
- 722 46. Tillich, M. *et al.* GeSeq – versatile and accurate annotation of organelle genomes.
723 *Nucleic Acids Research* **45**, W6–W11 (2017).
- 724 47. Chan, P. P. & Lowe, T. M. tRNAscan-SE: Searching for tRNA genes in genomic
725 sequences. *Methods Mol Biol* **1962**, 1–14 (2019).
- 726 48. Laslett, D. & Canback, B. ARAGORN, a program to detect tRNA genes and tmRNA
727 genes in nucleotide sequences. *Nucleic Acids Research* **32**, 11–16 (2004).
- 728 49. Laslett, D. & Canbäck, B. ARWEN: a program to detect tRNA genes in metazoan
729 mitochondrial nucleotide sequences. *Bioinformatics* **24**, 172–175 (2008).
- 730 50. Sallet, E., Gouzy, J. & Schiex, T. EuGene: An Automated Integrative Gene Finder for

- 731 Eukaryotes and Prokaryotes. in *Gene Prediction: Methods and Protocols* (ed. Kollmar, M.) 97–
732 120 (Springer, New York, NY, 2019). doi:10.1007/978-1-4939-9173-0_6.
- 733 51. Howe, K. L., Bolt, B. J., Shafie, M., Kersey, P. & Berriman, M. WormBase ParaSite –
734 a comprehensive resource for helminth genomics. *Mol Biochem Parasitol* **215**, 2–10 (2017).
- 735 52. UniProt Consortium, T. UniProt: the universal protein knowledgebase. *Nucleic Acids*
736 *Res* **46**, 2699 (2018).
- 737 53. Bao, W., Kojima, K. K. & Kohany, O. Repbase Update, a database of repetitive
738 elements in eukaryotic genomes. *Mobile DNA* **6**, 11 (2015).
- 739 54. Wang, Y. *et al.* MCScanX: a toolkit for detection and evolutionary analysis of gene
740 synteny and collinearity. *Nucleic Acids Res* **40**, e49 (2012).
- 741 55. Sun, L., Zhuo, K., Lin, B., Wang, H., & Liao, J. Meloidogyne graminicola
742 mitochondrion, complete genome. Available at:
743 https://www.ncbi.nlm.nih.gov/nuccore/NC_056772.1. NCBI. National Center for
744 Biotechnology Information (2014).
- 745 56. Humphreys-Pereira, D. A. & Elling, A. A. Meloidogyne arenaria mitochondrion,
746 complete genome. Available at: https://www.ncbi.nlm.nih.gov/nuccore/NC_026554.1.
747 National Center for Biotechnology Information (2015).
- 748 57. Humphreys-Pereira, D. A. & Elling, A. A. Meloidogyne javanica mitochondrion,
749 complete genome. Available at: https://www.ncbi.nlm.nih.gov/nuccore/NC_026556.1.
750 National Center for Biotechnology Information (2015).
- 751 58. Humphreys-Pereira, D. A. & Elling, A. A. Mitochondrial genomes of Meloidogyne
752 chitwoodi and M. incognita (Nematoda: Tylenchina): Comparative analysis, gene order and
753 phylogenetic relationships with other nematodes. *Molecular and Biochemical Parasitology*
754 **194**, 20–32 (2014).
- 755 59. Besnard, G. *et al.* On the close relatedness of two rice-parasitic root-knot nematode
756 species and the recent expansion of Meloidogyne graminicola in Southeast Asia. *Genes*, 10(2),
757 175. <https://doi.org/10.3390/genes10020175> (2019).
- 758 60. Zijlstra, C., Donkers-Venne, D. T. H. M. & Fargette, M. Identification of Meloidogyne
759 incognita, M. javanica and M. arenaria using sequence characterised amplified region (SCAR)
760 based PCR assays. *Nematology* **2**, 847–853 (2000).
- 761 61. European Nucleotide Archive. <https://identifiers.org/ena.embl:PRJEB69523>. (2024).
- 762 62. Pouillet Marine & Danchin Etienne G. J. Meloidogyne enterolobii assemblies.
763 Recherche Data Gouv <https://doi.org/10.57745/5MXZSJ> (2023).
- 764 63. Pouillet Marine, Danchin Etienne G. J, & Rancurel Corinne. Meloidogyne enterolobii
765 E1834 gene prediction. Recherche Data Gouv <https://doi.org/10.57745/Y0O2LP> (2023).
- 766 64. Pouillet Marine & Danchin Etienne G. J. Meloidogyne enterolobii E1834 structural
767 annotation. Recherche Data Gouv <https://doi.org/10.57745/VEKHQS> (2023).

- 768 65. Jaron, K. S. *et al.* Genomic Features of Parthenogenetic Animals. *Journal of Heredity*
769 **112**, 19–33 (2021).
- 770 66. Liu, B. *et al.* Estimation of genomic characteristics by analyzing k-mer frequency in de
771 novo genome projects. Preprint at <https://doi.org/10.48550/arXiv.1308.2012> (2020).
- 772 67. Quinlan, A. R. & Hall, I. M. BEDTools: a flexible suite of utilities for comparing
773 genomic features. *Bioinformatics* **26**, 841–842 (2010).
- 774 68. Manni, M., Berkeley, M. R., Seppey, M., Simão, F. A. & Zdobnov, E. M. BUSCO
775 Update: Novel and Streamlined Workflows along with Broader and Deeper Phylogenetic
776 Coverage for Scoring of Eukaryotic, Prokaryotic, and Viral Genomes. *Molecular Biology and*
777 *Evolution* **38**, 4647–4654 (2021).
- 778 69. Lunt, D. H. Genetic tests of ancient asexuality in Root Knot Nematodes reveal recent
779 hybrid origins. *BMC Evol Biol* **8**, 194 (2008).
- 780
- 781